

Article

Projected Crop Production under Regional Climate Change Using Scenario Data and Modeling: Sensitivity to Chosen Sowing Date and Cultivar

Sulin Tao ¹, Shuanghe Shen ^{1,*}, Yuhong Li ^{2,†}, Qi Wang ^{3,†}, Ping Gao ⁴ and Isaac Mugume ⁵

¹ Collaborative Innovation Centre on Forecast and Evaluation of Meteorological Disasters, School of Applied Meteorology, Nanjing University of Information Science & Technology, Nanjing 210044, China; sulin.tao@outlook.com

² Liaoning Institute of Meteorological Sciences, Shenyang 110166, China; liyh0609@163.com

³ National Meteorological Information Centre, Beijing 100081, China; qiawang@cma.gov.cn

⁴ Meteorological Service Centre for Jiangsu Province, Nanjing 210008, China; gaoping5268@126.com

⁵ Department of Geography, Geo-Informatics & Climatic Sciences, Makerere University, P.O. Box 7062, Kampala, Uganda; imugume@caes.mak.ac.ug

* Correspondence: yqzhr@nuist.edu.cn; Tel.: +86-025-58731011

† These authors contributed equally to this work.

Academic Editor: Kevin Murphy

Received: 7 December 2015; Accepted: 23 February 2016; Published: 27 February 2016

Abstract: A sensitivity analysis of the responses of crops to the chosen production adaptation options under regional climate change was conducted in this study. Projections of winter wheat production for different sowing dates and cultivars were estimated for a major economic and agricultural province of China from 2021 to 2080 using the World Food Study model (WOFOST) under representative concentration pathways (RCPs) scenarios. A modeling chain was established and a correction method was proposed to reduce the bias of the resulting model-simulated climate data. The results indicated that adjusting the sowing dates and cultivars could mitigate the influences of climate change on winter wheat production in Jiangsu. The yield gains were projected from the chosen sowing date and cultivar. The following actions are recommended to ensure high and stable yields under future climate changes: (i) advance the latest sowing date in some areas of northern Jiangsu; and (ii) use heat-tolerant or heat-tolerant and drought-resistant varieties in most areas of Jiangsu rather than the currently used cultivar. Fewer of the common negative effects of using a single climate model occurred when using the sensitivity analysis because our bias correction method was effective for scenario data and because the WOFOST performed well for Jiangsu after calibration.

Keywords: bias correction; WOFOST model; regional climate change; representative concentration pathways scenarios; adaptation options; winter wheat; Jiangsu

1. Introduction

The mechanisms underlying the impacts of climatic change and variability on crop production are very complex. Continued global warming and increased climate variability might result in greater high-temperature stress and unstable agro-climatic resources. Slight variations in the mean climate (e.g., temperature and precipitation) might lead to asymmetrical responses in the frequency and intensity of severe weather events that cause high or low temperature injuries, large-scale droughts or severe floods that further reduce crop yields [1,2]. However, the positive effects of climate change are undeniable, especially at regional scales. Increases in precipitation, relative humidity and carbon dioxide concentrations will contribute to increased crop yields. Increases in temperature may also

increase crop yields, particularly where the initial temperature is low [3]. The interactions of crops, climate and soil are responsible for the complicated impacts of climate change on crop production.

Regional climatic change and variability sometimes lag behind global climate warming trends, particularly in regions that are influenced by several weather systems. Local assessment is required to map the adaptations of cultivation areas to climate change, and crop models are effective for evaluating the responses of crop production to climate change and variability [4]. The influences of climate on winter wheat productivity in 50 ecological zones of China were evaluated using the World Food Study model (WOFOST), which indicated positive effects in northern regions and negative effects in southern regions [5]. Regional climate models (RCMs) driven by general circulation models (GCMs) facilitate the assessment of regional impacts. By using the Decision Support System for Agrotechnology Transfer (DSSAT) with climate change scenarios derived from Providing Regional Climates for Impacts Studies (PRECIS), the negative impacts of increased temperature on wheat yield were determined in the sub-mountainous region of the Punjab state of India [6]. In addition, satellite-derived data were used to facilitate local assessments. The improved yield simulations would benefit from the assimilation of the green area index with 250-m MODIS pixels into the WOFOST model [7]. The potential effects of climate change and variability on crop production were also evaluated by Riha [8], Hulme [9] and Semenov *et al.* [10].

However, for agricultural sustainable development, suitable measures for facilitating adequate adaptation to climate change must be evaluated using local assessments. Cuculeanu *et al.* [11] demonstrated that using appropriate maize hybrids, sowing dates, crop densities and fertilizer application rates could decrease the adverse impacts of the Romanian climate. Torriani *et al.* [12] projected the responses of maize yield to different cultivars with different accumulated thermal units and sowing dates and demonstrated the benefits of using higher thermal time requirements and shifting sowing dates in Switzerland. The sensitivities of crop production to adaptations were also evaluated by Alexandrov [13], Luo [14] and Olesen *et al.* [15]. Nonetheless, the potential responses of crops to varying adaptation options are crop- and region-specific, and the cropping patterns used by individual farmers are unlikely to change in the immediate future [16]. Thus, more rigorous, persuasive and specific assessments of adaptation options are required.

The rigorous evaluation of options for adapting to regional climate change requires reliable and high resolution (e.g., 0.5° latitude by 0.5° longitude) simulations of future climates (including temperature, precipitation, radiation and other elements). Dynamical downscaling methods relying on output from RCMs coupled with GCMs frequently provide sufficiently accurate future climate simulations. The credibility of these methods mainly results from the descriptions of mean values, extremes, variability, seasonal cycles and other statistics. However, dynamical downscaling has limitations [17,18], which are impossible to avoid when improving simulation resolutions. Some bias correction and downscaling treatments are still required for the simulations.

Statistical downscaling to identify statistical relationships between predictors (the outputs from GCMs) and predictands (the required variables) [19] could be used to construct a bias correction method based on historical observations. This method should consider the inaccuracies in the descriptions of the seasonal and monthly distributions of climate elements in future scenarios due to scenario validation at the annual scale. Acceptable trends and weak bias can be obtained when comparing present climate simulations and observations from the perspective of annual validation; however, these trends may not persist at seasonal or monthly scales. Two additional issues should be considered: (i) variations of climate elements at the daily scale might strongly influence crop growth; and (ii) the accuracy of simulated winter warming is very important for winter crop research. Bakker *et al.* [20] suggested using bias corrections when applying RCM outputs and examined their efficiencies extensively.

Reduced low temperature stress was found in irrigated rice, but no increases in high temperature stress was found during global warming in China from 1961 to 2008 [21]. Winter crops are also affected by a warming climate, particularly in local regions with variable climates. The main objective of this

study is to establish a modeling chain for estimating the projections of crop production using scenario data. In this study, a partial sustainability assessment of the local agricultural economy is conducted. A sensitivity analysis of crop production responses to chosen sowing dates and cultivars is conducted, and suitable sowing dates and winter wheat varieties for sustainable agricultural development are identified for a major economic and agricultural province of China. Using a single climate model results in methodological limitations. However, these limitations could be reduced for sensitivity analysis. Moreover, a bias correction method is introduced to reduce shifts in the mean climate and climate variability in future scenarios to ensure the reliability of the projections.

2. Methodology

2.1. Study Region

This study was conducted in Jiangsu Province along the eastern coast of China and west of the Yellow Sea (Figure 1a). This region has a variable climate due to large-scale and internal forcing, including a subtropical high-pressure system and the East Asian monsoon and land-sea distributions. The subtropical monsoon dominates the climate in the southern areas, and the warm moist monsoon dominates the climate in the northern areas. The weather is mild throughout the region, with moderate rainfall and a clear distinction between the four seasons. The annual average temperature ranges from 13.0~16.5 °C within this region, and the temperatures in the Huaibei (the Yellow River and Huai River), Jianghuai (the Yangtze River and Huai River) and southern Jiangsu regions range from 13.0~14.0 °C, 14.0~15.0 °C, and 15.0~16.5 °C, respectively [22]. Precipitation in the region increases from northwest to southeast, and the average annual precipitation is 800~1200 mm, with 60% of the precipitation occurring during the summer [22].

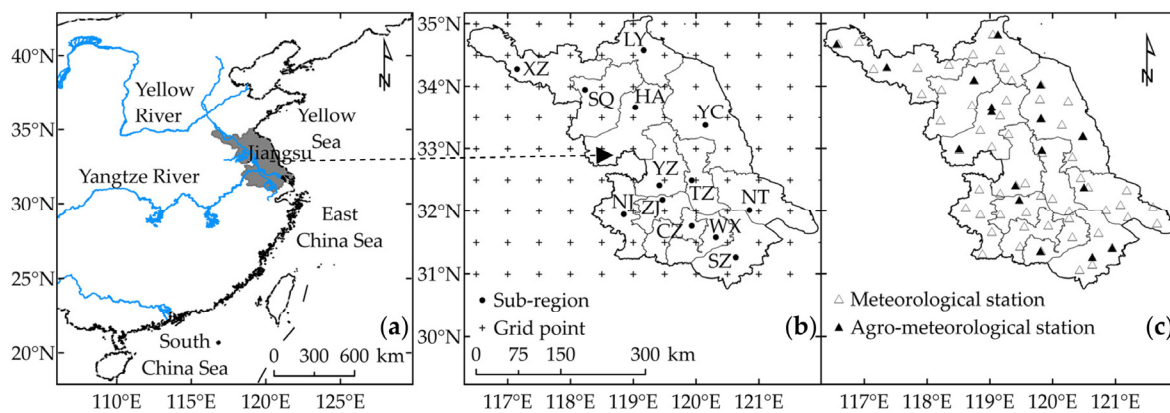


Figure 1. (a) Location of Jiangsu Province in the eastern coastal area of China; (b) Locations of sub-regions and grid points; (c) Locations of meteorological stations and agro-meteorological stations. CZ stands for Changzhou, HA stands for Huaian, LY stands for Lianyungang, NJ stands for Nanjing, NT stands for Nantong, SQ stands for Suqian, SZ stands for Suzhou, TZ stands for Taizhou, WX stands for Wuxi, XZ stands for Xuzhou, YC stands for Yancheng, YZ stands for Yangzhou, and ZJ stands for Zhenjiang. The Huaibei region covers the areas of XZ, LY, and SQ and the northern parts of HA and YC. The Jianghuai region covers the areas of NT, TZ, YZ, the northern parts of NJ, and the southern parts of YC and HA. The southern Jiangsu region covers the areas of SZ, WX, CZ, ZJ and the southern parts of NJ.

Winter wheat production plays an important role in the gross output of Jiangsu. Winter wheat is planted in all of the sub-regions in this province (Figure 1b). From 2011 to 2013, the output of winter wheat accounted for approximately 30.93%~32.17% of the total grain production in this region and 9.17%~9.51% of the planting area in China [23]. However, in this economic and agricultural region, winter wheat production faces the following two challenges:

- (i) The scarcity of cultivated land resources. As the economics in the province develop, the demand for non-farming construction land increases. Large areas of cultivated land have been transformed into construction land due to urbanization. The southern part of the province has a lower average amount of cultivated land per person than the northern region and a more rapid rate of decreasing farm land area [24].
- (ii) Observed climate change. Since 1961, the climate of this region has undergone successive cooling and warming periods. However, during recent decades, a significant warming trend has persisted. The average temperature from 2001 to 2006 increased by 1.0 °C compared with the average temperature from 1971 to 2000 [24]. However, the extent of warming varies over smaller spatial scales. The temperature is 0.9 °C greater over the Huaibei region and Jianghuai region and 1.2 °C greater over the southern Jiangsu region [24].

The precipitation in the province has decreased since the mid-1990s with significant annual fluctuations. The Meiyu season results in a complex pattern of precipitation due to the timing, position and duration of the rain belt. The northward movement of this rain belt increases precipitation in the Huaibei region and decreases precipitation in the southern Jiangsu region [24].

The observed climate change has influenced winter wheat production in Jiangsu. Thirty-seven to 41% of the wheat yield in this province from 1978 to 1995 can be explained by temperature variations, and the negative impacts of the changes in seasonal average temperature (at the provincial scale) and total precipitation (at a 0.5° scale) on wheat yield are evident [25]. The variations of the climate change present at different spatial scales increase the challenge of investigating the impacts of climate change and variability on wheat production.

2.2. Data

New emission scenarios of the representative concentration pathways (RCPs) were used in this study. The RCPs consist of four scenarios, RCP2.6, RCP4.5, RCP6 and RCP8.5, which have been updated from earlier scenarios using more detailed information, including emission, concentration and land-use trajectory data and several climate policies and adaptations. RCP8.5 and RCP2.6 represent a very high and low forcing level and stabilize the radiative forcing at approximately 1370 and 490 ppm CO₂-equivalents, respectively, in 2100 [26,27]. RCP6 and RCP4.5 represent two medium stabilization scenarios and stabilize the radiative forcing at approximately 850 and 650 ppm CO₂-equivalents, respectively, in 2100 [26,28].

Of these RCPs, RCP4.5 is the most consistent with future development in eastern China, where improvements in energy structure and new low-emission technologies that limit emissions are most likely conducted. Projections from the RCP8.5 scenario in the absence of climate policies are also valuable as comparisons. Moreover, the land use projections are first considered in the RCPs, and the RCP4.5 and RCP8.5 scenarios produced two relevant, typical patterns of future land use. Evident areas of high-density cropland are projected in RCP8.5 in Southeast Asia and secondary (recovering) vegetation is projected to be common in Eurasia by 2100; however, less cropland, more land with no fractional cropland and high-density areas of secondary vegetation are projected in RCP4.5 [26].

Climate scenario data from RCP4.5 and RCP8.5 from 2021 to 2080 (60 years) and present climate data (historical simulations) from 1961 to 2005 (45 years) with a resolution of 0.5° latitude by 0.5° longitude (approximately 50 km × 50 km) were created using the outputs of the Beijing Climate Centre Climate System Model version 1.1 (BCC_CSM1.1, a Chinese model) as the initial and boundary conditions to drive the regional climate model of the International Centre for Theoretical Physics (RegCM4.0) [27–29]. The elements of the grid points (Figure 1b) included the daily mean temperature (T , °C), maximum temperature (T_{max} , °C), minimum temperature (T_{min} , °C), wind speed (UV , $m \cdot s^{-1}$), precipitation (P , mm) and radiation (R , $w \cdot m^{-2}$).

The climate observations from 1961 to 2005 (45 years) of the 60 meteorological stations (Figure 1c) were provided by the Jiangsu Meteorological Information Centre and included the daily mean temperature (T , °C), maximum temperature (T_{max} , °C), minimum temperature (T_{min} , °C),

precipitation (P , mm), wind speed (UV , $m \cdot s^{-1}$) and sunshine duration (S , h). The observed phenology and yield data from 1991 to 2005 (15 years) of the 17 agro-meteorological stations (Figure 1c) were also used.

Soil parameters for each meteorological station, including the sand fraction ($\% g \cdot g^{-1}$) and clay fraction ($\% g \cdot g^{-1}$) of topsoil (0–30 cm) and subsoil (30–100 cm), were extracted from the Harmonized World Soil Database (HWSD) using a resolution of approximately $1 km \times 1 km$ [30].

2.3. Modeling Framework

2.3.1. The Crop Growth Model

Before the crop simulations were performed, a bias correction method for model-simulated climate data at the daily scale was proposed based on statistical downscaling for the shifts in the mean climate and climate variability in the climate scenarios. This method was applied to daily values to adjust the mean and variance. The main steps of this method can be found in the Appendix. Its effectiveness was verified using simulated climate data and observed data during the validation period of 1991–2005. This method was then used to correct future climate data under the RCP scenarios for 2021–2080.

The crop growth and soil water balance were then simulated using the World Food Study model (WOFOST) with a daily time step [31,32]. WOFOST is a mechanistic crop growth model with a solid biophysical and ecological basis. This model can simulate many crops by changing the crop parameters. The major processes for crop growth are phenological development, CO_2 -assimilation, transpiration, respiration, partitioning of assimilates to various organs, and dry matter formation. The major processes for water balance are rainfall, surface storage, surface run-off, soil surface evaporation, crop transpiration, percolation from the root zone to deeper layers and capillary rise into the root zone. This model can be applied using the potential mode (driven solely by solar radiation and temperature) and the water-limited mode (limited by the availability of water).

Although the WOFOST model was developed mainly for Europe, it has been widely used to assess crop responses to climate change. The performances of the WOFOST model and seven other well-documented models (including APES, CROPSYST, DAISY, DSSAT, FASSET, HERMES and STICS) were compared for winter wheat in Europe. This comparison demonstrated that none of the models could always reproduce the actual reported observations perfectly and that WOFOST overestimated the winter wheat yield [33]. Nevertheless, in China, after extensive parameter calibration or the introduction of other techniques (e.g., satellite-driven data), good agreement was achieved between the observations and the simulations from WOFOST [34–36]. In this study, weather data and model parameters underwent bias correction and calibration, respectively, to improve the reliabilities of the projections. In addition, the WOFOST model should be reasonable for conducting the sensitivity analysis.

The winter wheat phenology parameters were calibrated using the observed phenology and meteorological data, and the assimilation and respiration characteristics and partitioning of assimilates to plant organs were derived from the WOFOST41 dataset [37].

The temperature sums from sowing to emergence, from emergence to anthesis and from anthesis to maturity ($^{\circ}C \cdot d$) were determined relative to the current cultivars using the observed phenology and meteorological data for the periods of 1993–1994, 1995–1996, 1996–1997 and 1999–2000 at the Fengxian, Shuyang, Ganyu, Binghai, Jianhu, Dafeng, Xinghua, Yangzhou and Rugao agro-meteorological stations. The detailed calibration steps include the following:

- (i) First, the average sowing, emergence, anthesis and maturity dates were calculated using the observed winter wheat phenology data from the agro-meteorological stations.
- (ii) Second, the temperature sums were calculated using the average phenology dates and meteorological data from each agro-meteorological station.

- (iii) Finally, the temperature sums from sowing to emergence, from emergence to anthesis and from anthesis to maturity over the entire study region were interpolated from the results of Step (ii). For a very flat region (*i.e.*, Jiangsu, most of which is within 50 m of sea level), it was reasonable to consider only the distances of the known points to the unknown points. In addition, because we aim to preserve the known values (*i.e.*, observations) after spatial interpolation, a deterministic method is required. Thus, the inverse distance weights method was used.

Physical soil characteristic parameters, including the soil moisture content at wilting point ($\% \text{ cm}^3 \cdot \text{cm}^{-3}$), soil moisture content at field capacity ($\% \text{ cm}^3 \cdot \text{cm}^{-3}$), soil moisture content at saturation ($\% \text{ cm}^3 \cdot \text{cm}^{-3}$) and the hydraulic conductivity of the saturated soil ($\text{cm} \cdot \text{d}^{-1}$), were estimated using the module Soil-Water-CharacTeristics (SWCT) of the Soil-Plant-Air-Water (SPAW) model [38] with inputs (sand and clay fraction) from HWSD.

The WOFOST model was validated by comparing the simulated growth stages and yields to observations from 1992 to 1993, 1994 to 1995, 1997 to 1999 and 2001 to 2005 for the 7 stations (observed yields at Fengxian and Jianhu were not available) and from 1992 to 2005 for the other 8 stations.

2.3.2. Simulation Schemes

Historical and future simulations were performed in this study for comparison. Historical simulations of the present climate from 1961 to 1990 were considered as a baseline, and the simulations for each 30-year period, including 2021 to 2050 and 2051 to 2080, were used to obtain projections under future climate conditions.

Water-limited production levels were considered to investigate the responses of winter wheat to climatic variability in the RCP4.5 and RCP8.5 climate change scenarios because water-limited production levels represent the maximum yield obtained under rain-fed conditions. The management parameters were held constant, and the mean sowing dates for each 30-year period and conditions with no irrigation and fertilization were considered. Using these settings, the climate factors only influenced the winter wheat production when the variety was also held constant.

Our numerical simulations consisted of the following:

- (i) Running the WOFOST model under baseline and climate scenarios with average sowing dates according to the historical phenology and quantifying the changes in the winter wheat growing season, water use efficiency and water-limited yields.
- (ii) Running the WOFOST model under climate scenarios with varying sowing dates for 2021–2050 and 2051–2080. In theory, the last date at which the daily mean temperature consistently exceeded $15\text{ }^{\circ}\text{C}$ is treated as the latest optimal sowing date in Jiangsu. Next, the varying sowing dates for each site were established based on this date using shifts of 5 days. Sixty-day leads and 30-day lags from this date were defined as the inferior limit and superior limit of the possible sowing date interval, respectively. This varying range covered the current sowing dates (historical observations).
- (iii) Running the WOFOST model under climate scenarios with varying winter wheat varieties. Extreme events, such as heat stress and drought stress, may have major impacts on winter wheat yield [39,40]. Accordingly, heat-tolerant and drought-resistant varieties were considered in this study.

In the WOFOST model, crops die because they exceed the crop-specific life span in the heat stress situation, which is defined by the SPAN parameter at a constant temperature. Moreover, as a plant adapts its water potential to maintain potential transpiration in a water limited situation, a reduction factor is used in the WOFOST model to reduce the potential transpiration. Corresponding with this reduction factor, the DEP NR parameter that represents the crop group number for soil water depletion is defined from 1 (drought sensitive) to 5 (drought resistant). Thus, the values of SPAN and DEP NR

parameters can be changed to prepare heat tolerant and drought resistant varieties, respectively (Table 1).

Table 1. The proposed winter wheat varieties.

<i>Variety</i>	<i>Parameters</i>	<i>Characteristics</i>
V1	SPAN = 28.0 °C and DEP NR = 4.0	Current variety
V2	SPAN = 29.0 °C and DEP NR = 4.0	Heat tolerant
V3	SPAN = 30.0 °C and DEP NR = 4.0	Heat tolerant
V4	SPAN = 28.0 °C and DEP NR = 4.5	Drought resistant
V5	SPAN = 28.0 °C and DEP NR = 5.0	Drought resistant
V6	SPAN = 29.0 °C and DEP NR = 4.5	Heat tolerant and drought resistant
V7	SPAN = 29.0 °C and DEP NR = 5.0	
V8	SPAN = 30.0 °C and DEP NR = 4.5	
V9	SPAN = 30.0 °C and DEP NR = 5.0	

Finally, we sought to identify a suitable sowing date and variety for stable yields after the sensitivity analysis. We believe that selecting a sowing date (or a variety) from the possible sowing dates (or varieties) is likely optimal if all of the following conditions are satisfied, regardless of whether the chosen date (or variety) results in the maximum winter wheat yield.

- The minimum coefficient of variation (CV, the ratio of the standard deviation to the mean [41]) of the yield simulated using the possible sowing date (or variety) is less than or equal to the CV of the yield of the current sowing date (or variety).
- The simulated yield is greater than or equal to the yield simulated using the current sowing date (or variety).
- If more than one minimum is present, the CV results are equivalent, and the date (or variety) corresponding to the maximum yield is considered optimal.

The CV shows the extent of variability related to the mean. A small CV indicates a largely stable variable sequence.

3. Results

3.1. Effectiveness of the Bias Correction Method

Our bias correction model was applied to correct simulated climate data from 1991 to 2005, and the effectiveness of the model was evaluated. Then, the relative errors of the simulated elements compared with the climate observations were calculated at the monthly scale before and after bias correction (BC).

The bias between historical simulations and observations in different months was reduced for all six elements (Figure 2). Before BC, the differences between the simulations and observations during the winter (from December to February) were generally larger than the differences between the simulations and observations during the other three seasons. This behavior was more obvious for T and Tmin. The relative errors of P during the spring and R during the autumn and winter also indicated large discrepancies, and most of the unsatisfied simulations were constructions for UV during all four seasons. After BC, the discrepancies of these elements decreased, especially for T and Tmin during the winter and UV during all seasons. The relative errors of Tmax, P and R were low (approximately 0.2). The bias of the simulated temperature, radiation, and wind speed in the autumn and winter and the amount of precipitation in the winter and spring were markedly reduced.

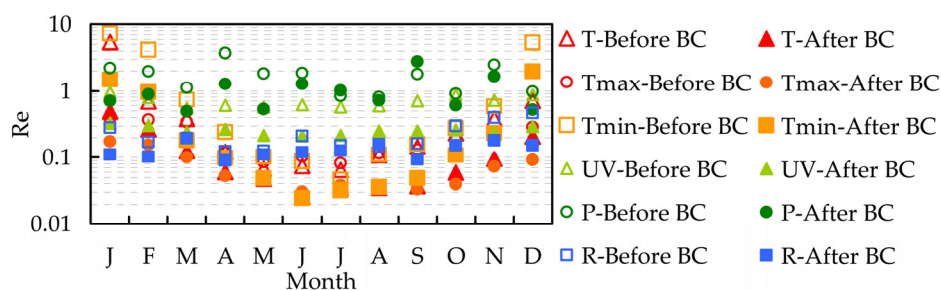


Figure 2. Relative error (Re) of the simulated mean temperature (T), maximum temperature (Tmax), minimum temperature (Tmin), wind speed (UV), amount of precipitation (P), and radiation (R) and their corrected values compared with observations during 1991–2005. BC represents bias correction.

Quantile-quantile plots were also introduced to provide evidence of the reliability of our method (Figure 3). The linearity of the points suggested that the corrections and observations of the maximum and minimum temperatures followed the same distribution. Our bias correction method was effective for correcting the elements under future climate scenarios. Thus, our method enhanced the credibility of the winter wheat production projections.

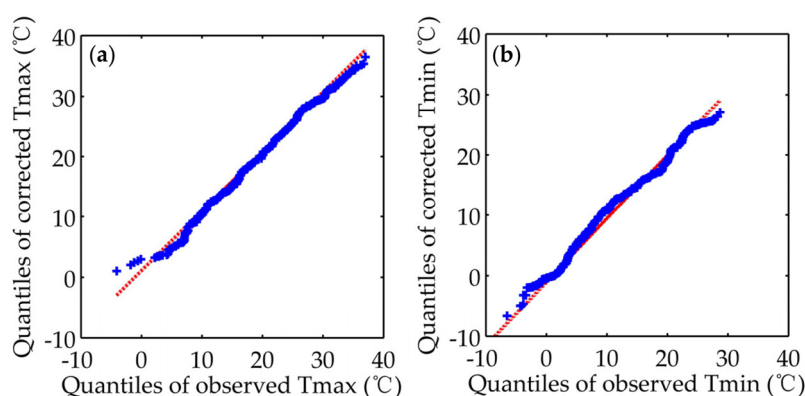


Figure 3. Quantile-quantile plot of the observed and corrected values of Nanjing in 1991: (a) Maximum temperature, Tmax; and (b) Minimum temperature, Tmin.

3.2. Calibration and Validation of WOFOST

The temperature sum parameters relative to the current winter wheat varieties and the physical soil characteristic parameters for each meteorological station in Jiangsu were calibrated as follows:

- (i) The temperature sums from sowing to emergence, from emergence to anthesis, and from anthesis to maturity ranged from 80.0 to 140.0 °C·d, 1380.0 to 2000.0 °C·d, and 600.0 to 800.0 °C·d, respectively. Higher temperature sums from sowing to emergence and from emergence to anthesis were required by the winter wheat in northern Jiangsu than in southern Jiangsu. However, lower temperature sums from anthesis to maturity were required by winter wheat in northern Jiangsu compared with southern Jiangsu.
- (ii) The dominant soil groups within the province include Acrisols, Alisols, Anthrosols, Fluvisols, Gleysols, Luvisols, Planosols, Regosols, Solonchaks and Vertisols. In most areas of the province, the soil moisture contents at the wilting point, field capacity and saturation ranged from 4.7% to 33.3% $\text{cm}^3 \cdot \text{cm}^{-3}$, 9.7% to 44.6% $\text{cm}^3 \cdot \text{cm}^{-3}$ and 44.8% to 52.0% $\text{cm}^3 \cdot \text{cm}^{-3}$, respectively. The hydraulic conductivities of the saturated soil varied from 2.1 to 277.2 $\text{cm} \cdot \text{d}^{-1}$ and were different in the different areas of the province. The various soil groups likely account for the complex spatial patterns of these soil parameters, especially over central and northern Jiangsu.

The simulated emergence dates were within $\pm 10\%$ of the observations (Figure 4a). The simulations of the anthesis and maturity dates were not as accurate as those of the emergence dates; however, most of the simulated dates for these two stages were within $\pm 10\%$ of the observations (Figure 4b,c). The simulated yields were slightly higher than the observations (Figure 4d). Some of the simulations exceeded the limit of $\pm 10\%$ but remained within $\pm 20\%$. This result may reflect the absence of meteorological damage, disease, insect pest activity and other types of damage from our simulation schemes. However, most of the simulated yields were within $\pm 10\%$ of the observations.

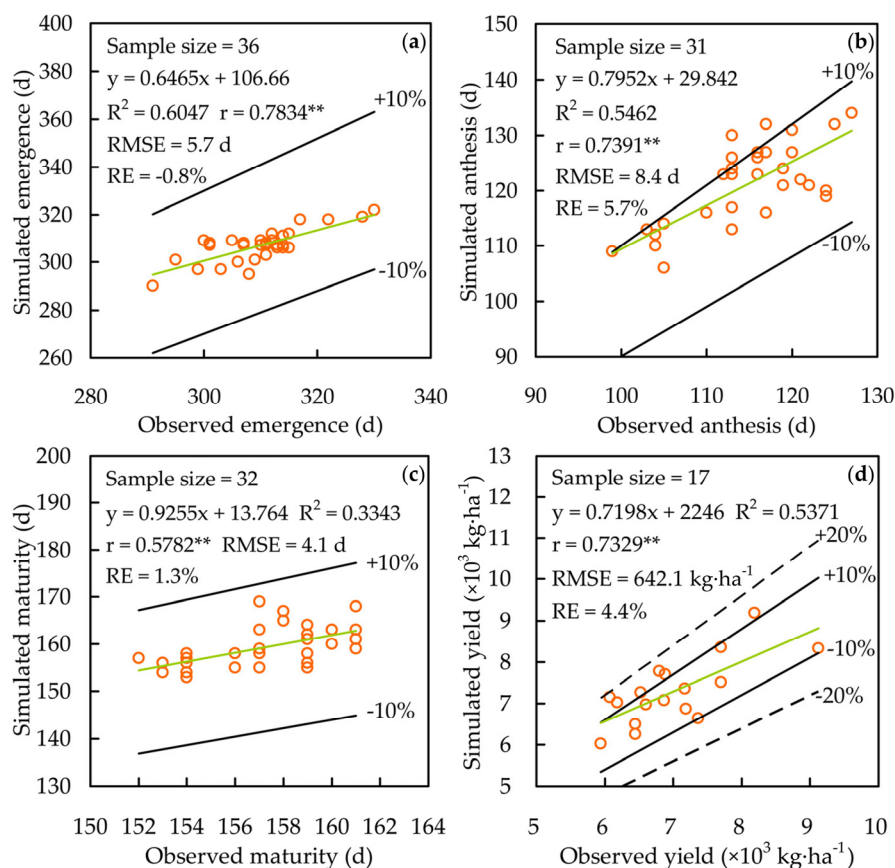


Figure 4. Comparisons of the simulated and observed: (a) emergence; (b) anthesis; (c) maturity; and (d) yield of winter wheat. The lime-colored solid line represents the regression line. Asterisks “***” indicate that the correlation is significant at the 0.01 level.

The following statistics were also included: the sample size, the linear regression, determination coefficient (R^2), correlation coefficient (r), Root Mean Square Error (RMSE) and Relative Error (RE). The RMSEs for the emergence, anthesis and maturity dates were 5.7 days, 8.4 days and 4.1 days, respectively. The RMSE for yield was $642.1 \text{ kg} \cdot \text{ha}^{-1}$. Generally, the WOFOST model with calibrated parameters was adequate for modeling winter wheat production in Jiangsu.

3.3. Corrected Climate Scenario Projections

The future climate in this province was projected to change from the baseline using the RCP4.5 and RCP8.5 scenarios. Generally, temperature and radiation were projected to increase, and wind speed and amount of precipitation were projected to decrease (Table 2). For temperature, the change for 2051–2080 was projected to exceed that of 2021–2050, especially in the RCP8.5 scenario. The changes in wind speed were small, and a greater change in precipitation was projected for 2021–2050 than for 2051–2080 in the RCP4.5 scenario. In addition, a greater change in radiation was found for 2051–2080 than for 2021–2050. These patterns are opposite of the patterns that were projected in the RCP8.5 scenario.

Table 2. Relative changes of future climate scenarios from the baseline.

Elements	1961–1990	2021–2050		2051–2080	
		RCP4.5	RCP8.5	RCP4.5	RCP8.5
T (°C)	14.77	+0.38	+0.42	+0.44	+0.63
Tmax (°C)	19.51	+0.30	+0.33	+0.30	+0.45
Tmin (°C)	11.10	+0.38	+0.42	+0.49	+0.71
UV (m·s ⁻¹)	2.97	Increase less than 0.01	Decrease less than 0.01	Decrease less than 0.01	Decrease less than 0.01
P (mm)	1578.05	−4.50	−0.79	−1.12	−6.04
R (MJ·m ⁻²)	4641.56	+13.86	+15.36	+15.08	+12.96

Climate change was obvious at the monthly scale under the projections. The climate elements increased from July to December and decreased during the other months. This behavior was much more pronounced for T, Tmax, Tmin and R than for the other elements (Figure 5a–c,f). Generally, these elements increased all year during 2051–2080 (Figure 5a–c). The monthly variations of UV and P were extensive. The UV decreased from March to October and increased from November to February. In addition, the P generally decreased but increased slightly in February, April, May, July, October, November and December. However, these two elements generally decreased (Figure 5d,e). The projected changes at the monthly scales could greatly influence the growth of winter wheat in this province.

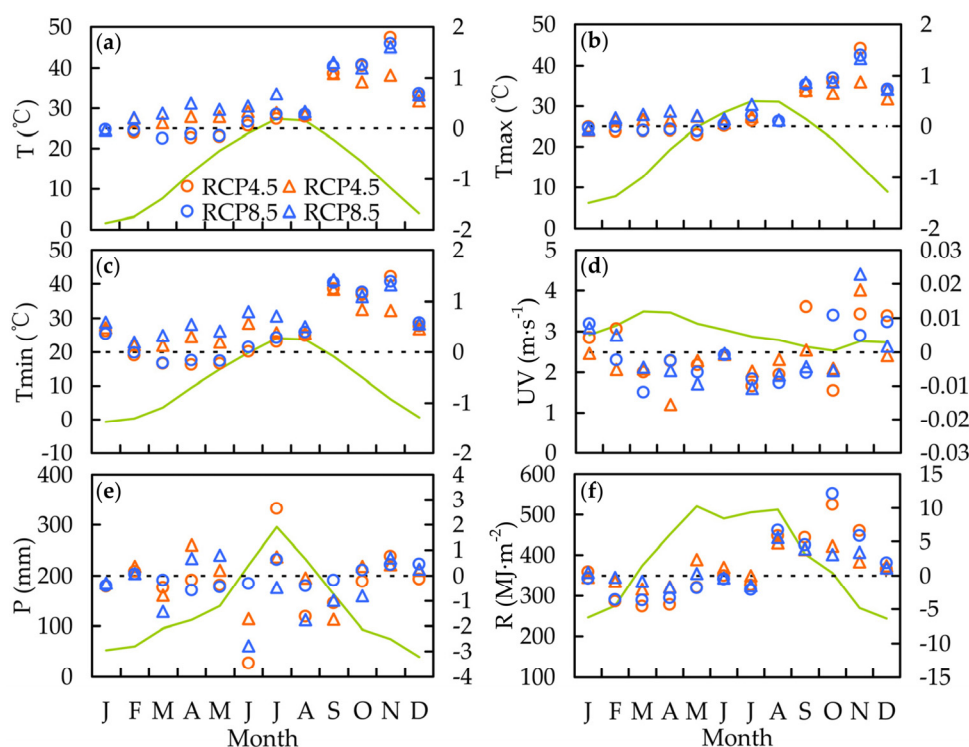


Figure 5. Relative changes of future climate scenarios from the baseline at the monthly scales: (a) Mean temperature; (b) Maximum temperature; (c) Minimum temperature; (d) Wind speed; (e) Amount of precipitation; and (f) Radiation. The lime-colored solid line represents the mean value of the climate element aggregated at the province level. The circle and triangle markers represent the changes during 2021–2050 and 2051–2080, respectively.

3.4. Projected Results from Using the Current Sowing Date and Cultivar

The growing season (GS), water use efficiency (WUE, the ratio of produced biomass to evapotranspiration rate) and water-limited yield were projected using the current sowing date and cultivar (Table 3).

Table 3. Winter wheat production under future climate scenarios compared with the baseline.

Variables	1961–1990	2021–2050		2051–2080		
		RCP4.5	RCP8.5	RCP4.5	RCP8.5	
GS	Mean (d)	222	220	220	219	218
	Standard deviation (d)	1.21	1.12	1.37	1.07	1.31
	CV (%)	0.54	0.51	0.62	0.49	0.60
	Trend (d·decade ⁻¹)	−0.48 ^a	−0.78 ^a	−0.59 ^a	−0.24	−0.72 ^a
WUE	Mean (kg·m ⁻³)	4.5	5.0	5.0	4.8	4.9
	Standard deviation (kg·m ⁻³)	0.117	0.179	0.174	0.164	0.178
	CV (%)	2.6	3.6	3.5	3.4	3.6
	Trend (kg·decade ⁻¹ ·m ⁻³)	−0.041 ^a	−0.046	−0.083 ^a	−0.036	0.036
Yield	Mean (kg·ha ⁻¹)	7239	7768	7714	7527	7613
	Standard deviation (kg·ha ⁻¹)	159	246	226	167	189
	CV (%)	9.8	9.9	9.9	9.7	9.8
	Trend (kg·decade ⁻¹ ·ha ⁻¹)	−36.4	−75.7	−154.4 ^a	−53.5	47.3

Note: Superscript lowercase “a” indicates a trend that exceeds a confidence level of 0.05.

Under the projections, the average GS under future climate scenarios became shorter compared with the average baseline in the province. In both the RCP4.5 and RCP8.5 scenarios, maturity occurred earlier, especially from 2051 to 2080. In general, the variability of GS was low, with a maximum standard variation of 1.37% and a CV of 0.62% for 2021–2050 in the RCP8.5 scenario. Although the GS generally became more stable in all scenarios, the most stable GS occurred in the RCP4.5 scenario relative to the baseline, and the least stable GS occurred in the RCP8.5 scenario. Moreover, the declining trends of the growing season were significant (according to the Mann–Kendall test) during both the baseline and future scenarios, except for 2051–2080 in the RCP4.5 scenario.

The winter wheat crops in this region used the available soil water more efficiently in the future climate scenarios. Although the average WUEs increased to some extent, the increases were greater for 2021–2050 than for 2051–2080. However, the standard deviation and CV indicate that the WUE was less stable in the future scenarios than in the baseline. In general, the WUE decreased for both 30-year periods and in both scenarios, except for the 2051–2080 period in the RCP8.5 scenario, in which the WUE increased.

The average winter wheat yields were projected to increase during future periods. In the RCP4.5 and RCP8.5 scenarios, the average yields were 409 kg·ha⁻¹ and 425 kg·ha⁻¹ higher, respectively, than the baseline. The variability of the yield was greater than that of GS and WUE and was generally higher during 2021–2050 and lower during 2051–2080 relative to the baseline. Decreasing trends of winter wheat yields were projected under both the baseline and RCP4.5 scenario. In contrast, in the RCP8.5 scenario, a significant decreasing trend was projected for 2021–2050, and an increasing trend was projected for 2051–2080.

Figure 6 presents the projected yields of 13 sub-regions in Jiangsu. The yields under the baseline in LY, NT, TZ and YC (mainly the coastal areas of Jiangsu) were high, with large medians, and relatively large inter-quartile yields were simulated in NT, which implied unstable production in this region. The simulated yields in CZ and NJ (mainly southwestern Jiangsu) were relatively low with small medians. Generally, the production in HA, LY, SQ and XZ (mainly northern Jiangsu) was relatively stable, with a small inter-quartile range for yields compared with the other sub-regions.

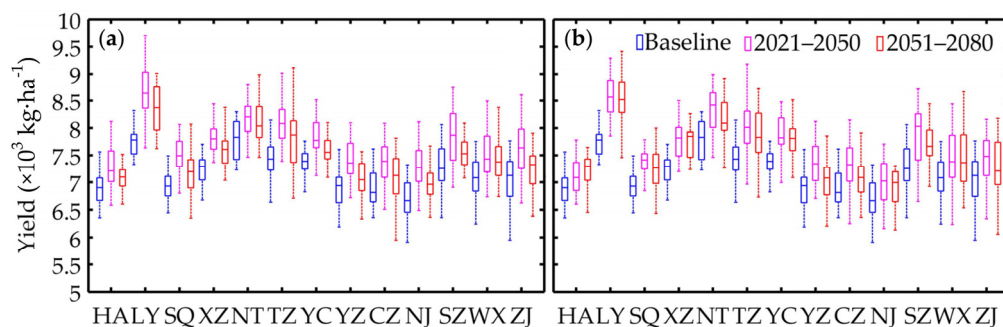


Figure 6. Distribution of the average projected yields of 13 sub-regions (see Figure 1) in the (a) RCP4.5 and (b) RCP8.5 scenarios. Boxes and whiskers represent the inter-quartile range (between the 25th and 75th percentiles) and maximum and minimum values, and the central mark represents the median.

Under future climate scenarios, the yield increases in LY (northeastern Jiangsu) were generally greater than the yield increases in the other sub-regions. However, a tendency towards unstable yields with expanded inter-quartile ranges was also projected in this sub-region. Large yield increases in TZ (central Jiangsu) were also projected, and a strong tendency towards unstable yields was projected with an expanded inter-quartile range and minimum-maximum range, especially during 2051–2080 in the RCP4.5 scenario. The projected yield changes were less obvious in other sub-regions. In addition, the yields in HA, NT, YC, NJ and SZ were projected to remain stable relative to the baseline during 2051–2080 in the two scenarios, and unstable yields were projected in the SQ. In the sub-regions WX and ZJ, a tendency towards stable yields was projected in the RCP4.5 scenario and a tendency towards unstable yields was projected in the RCP8.5 scenario. Trends that were not very obvious were projected in XZ, YZ and CZ.

Although the average winter wheat yields were projected to increase over most of Jiangsu during future periods, the change trends of each sub-region were generally very different from each other, especially under the different climate scenarios.

3.5. Sensitivities of the Projected Productions to the Chosen Sowing Date

The projections described above demonstrate that future climate conditions will affect winter wheat production in Jiangsu by influencing the growing season, water use efficiency and water-limited yield. Jiangsu is a major economic and agricultural province in China. Thus, policymakers should consider effective adaptations for stable and sustainable winter wheat production because most climate elements, especially temperature, are projected to markedly increase from July to December. Rigorous evaluations of relevant adaptation options were required.

The sensitivities of the projections to sowing date were evaluated using twenty possible sowing dates for each station. The current sowing dates were used as the possible sowing dates for evaluation. Three sites were selected for illustration, including Shuyang, Jianhu and Wuxi, which are located in the Huaibei, Jianghuai and southern Jiangsu regions, respectively. Figure 7 shows the high yield with small CV for winter wheat that was obtained from earlier sowing during 2021–2050 in the RCP4.5 and RCP8.5 scenarios. A clear decrease in yield and a clear increase in CV were projected due to late sowing.

The most suitable range of sowing dates for each site was determined according to Conditions (a)–(c) outlined in Section 2.3.2. The most suitable sowing date, as determined by a minimum CV and a high yield, was at least 25 days earlier than the last date on which the daily mean temperature consistently exceeded 15 °C. However, this result was obtained without considering the potential influences of other factors, such as disease, insect pest activity and fertilization. Thus, the most suitable sowing date identified here should be considered as an inferior limit, *i.e.*, the earliest sowing date, and the latest sowing date was the last date on which the daily mean temperature consistently exceeded 15 °C.

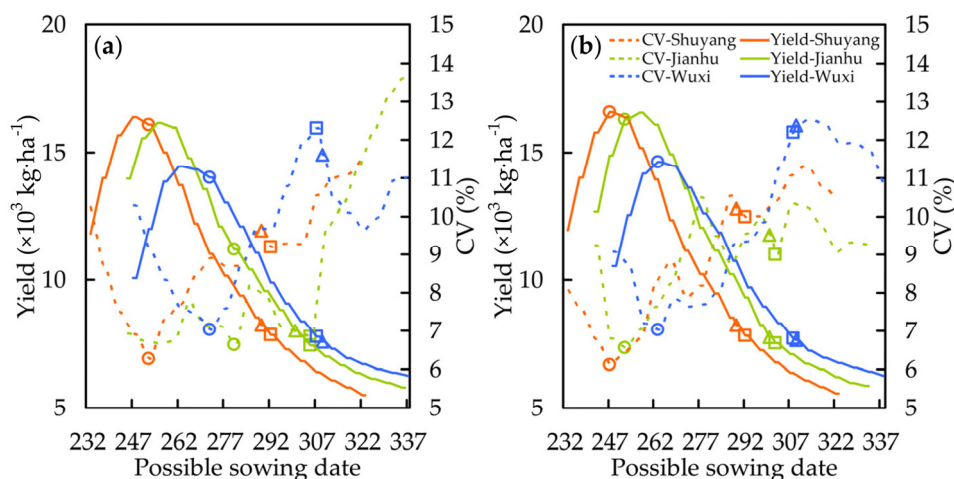


Figure 7. Sensitivity to the chosen sowing dates in the (a) RCP4.5 and (b) RCP8.5 scenarios during 2021–2050. The circles and squares represent the earliest and latest identified sowing dates, respectively. Triangles represent the current sowing date.

The ranges of the suitable sowing dates (bounded by a circle and square in Figure 7) for Shuyang, Jianhu and Wuxi were 41, 26 and 36 days, respectively, in the RCP4.5 scenario (Figure 7a). In the RCP8.5 scenario, the corresponding ranges were 46, 51 and 46 days, respectively (Figure 7b). The current sowing dates of Shuyang and Jianhu remained within their suitable ranges, whereas those of Wuxi were outside of the suitable range and far beyond the superior limit.

Next, the suitable ranges of sowing dates for obtaining stable yields in the other sub-regions were identified. The suitable sowing dates for the southern Jiangsu region were generally later than those for Jianghuai and Huaibei for each 30-year period (Figure 8). Some of the earliest sowing dates for the period of 2051–2080 were later than those of 2021–2050 in both the RCP4.5 and RCP8.5 scenarios (Figure 8b,d,f,h). In addition, some of the latest sowing dates were earlier, especially in the local areas of HA and XZ (Figure 8c,e,g,i). However, the suitable ranges identified in the RCP8.5 scenario differed from those in the RCP4.5 scenario. The main differences were the delays in both the earliest and latest sowing dates in the RCP8.5 scenario. Additionally, the current sowing dates for most parts of the Jianghuai region and the southern Jiangsu region remain within the suitable ranges, which indicates that these dates remain suitable during future periods. However, in the other regions, especially in the Huaibei region, the current sowing dates were not suitable to ensure stable production. For example, the identified suitable ranges included earlier sowing dates relative to the current dates in southwestern SQ and HA.

The yield gains projected from the application of the earliest sowing date were obvious (Figure 9). Large yield increases were projected in LY, SQ, XZ and NT for the earliest sowing date, while only small yield increases were projected in CZ and NJ. In addition, an obvious decrease in yield relative to the earliest sowing in HA was projected for 2051–2080 (Figure 9b,d). During the same period, a similar decrease was projected in SZ in the RCP8.5 scenario (Figure 9d). The yields, which were related to the latest and current sowing dates, were projected to be competitive yet different.

Changes in sowing date should be considered based on the relative positions of the yield medians related to the different sowing dates. However, the option of delaying the sowing date to produce high or stable wheat yields may not be practical for all regions as the climate becomes warmer. During 2021–2050, earlier sowing dates should be considered in HA, SQ and SZ in the RCP4.5 and RCP8.5 scenarios. In other sub-regions, the current sowing date was still suitable and could be slightly delayed (Figure 9a,c). Moreover, during 2051–2080 in the two scenarios, the earlier sowing date should be considered suitable in HA, SQ, XZ, NT and SZ and the current sowing date should be considered suitable in the other sub-regions (Figure 9b,d).

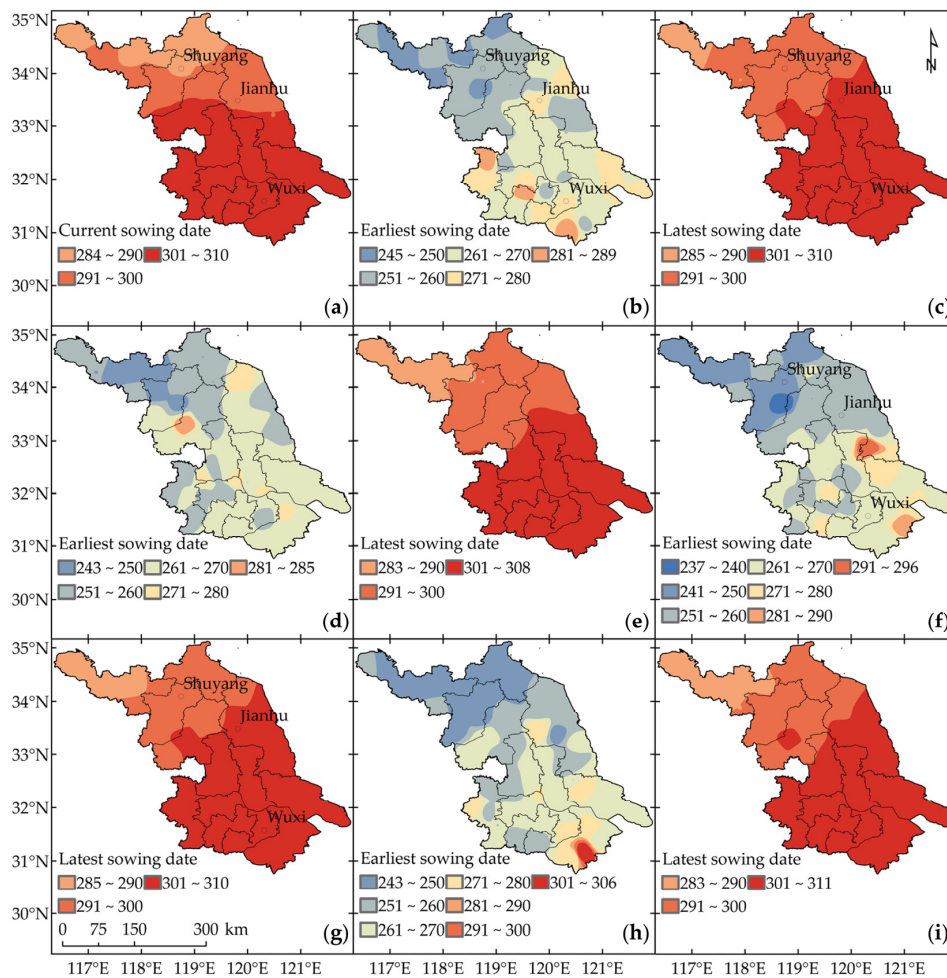


Figure 8. Suitable ranges of sowing dates for stable winter wheat yield under climate change scenarios: (a) Baseline; (b,c) RCP4.5 for 2021–2050; (d,e) RCP4.5 for 2051–2080; (f,g) RCP8.5 for 2021–2050; and (h,i) RCP8.5 for 2051–2080. Shuyang, Jianhu and Wuxi were labeled for illustration.

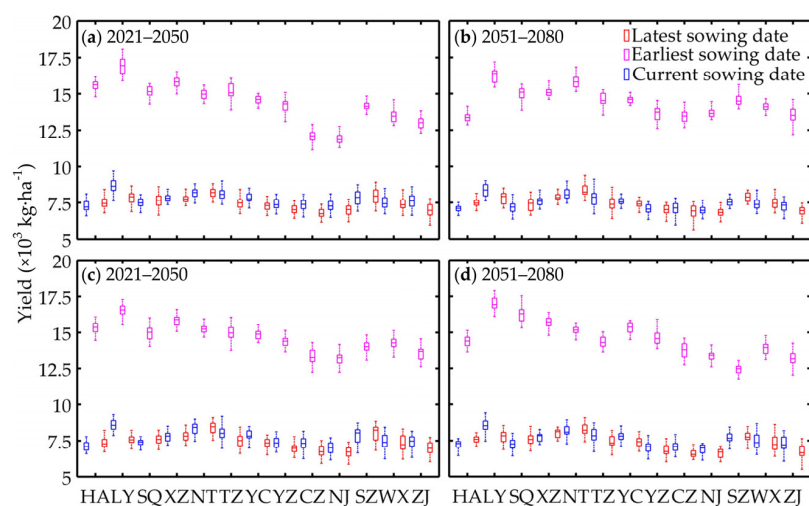


Figure 9. Distributions of average projected yields after using the identified suitable sowing dates in 13 sub-regions in the (a,b) RCP4.5 and (c,d) RCP8.5 scenarios. Boxes and whiskers represent the inter-quartile range (between the 25th and 75th percentiles) and maximum and minimum values, and the central mark represents the median.

3.6. Sensitivities of the Projected Productions to the Chosen Cultivar

Nine possible winter wheat varieties, including the current variety, were evaluated for each station. Three sites, including Shuyang, Jianhu and Wuxi, were selected for illustration. Figure 10 shows the high yields with small CVs for winter wheat that were obtained for heat-tolerant or heat-tolerant and drought-resistant varieties for 2021–2050 in the future climate scenarios. A clear decrease in yield was recognized because the SPAN and DEP NR decreased. In addition, adjusting only these two crop parameters would not result in great changes in the values of the yield CV.

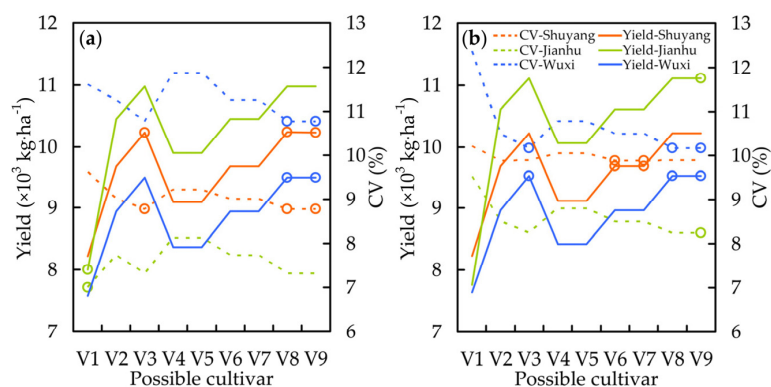


Figure 10. Sensitivity to the chosen cultivars in the (a) RCP4.5 and (b) RCP8.5 scenarios during 2021–2050. The circles represent the most suitable cultivars.

The most suitable variety was determined according to Conditions (a)–(c) outlined in Section 2.3.2. As determined by the minimum CV and high yield, the most suitable varieties for Shuyang included the heat-tolerant variety V3 and the heat-tolerant and drought-resistant varieties V8 and V9 in the RCP4.5 scenario. The current variety V1 was projected to be the most suitable for Jianhu, and the heat-tolerant and drought-resistant varieties V8 and V9 were projected to be the most suitable for Wuxi (Figure 10a). In the RCP8.5 scenario, the heat-tolerant and drought-resistant varieties V6 and V7 were projected to be most suitable for Shuyang, the heat-tolerant and drought-resistant variety V9 was projected to be most suitable for Jianhu, and the heat-tolerant variety V3 and the heat-tolerant and drought-resistant varieties V8 and V9 were projected to be most suitable for Wuxi.

Figure 11 shows the most suitable variety for each site. The heat-tolerant variety V3 and the heat-tolerant and drought-resistant varieties V8 and V9 were dominant among the high- and stable-yielding winter wheat cultivars.

For 2021–2050, the V1 variety remained the most suitable variety for northwestern XZ and other local areas, including northeastern LY, western CZ, SQ, WX and YC in the RCP4.5 scenario (Figure 11a) and southern and northern YZ, southern NT and TZ in the RCP8.5 scenario (Figure 11c). The resistant varieties, including the heat-tolerant variety V2, the drought-resistant varieties V4 and V5 and the two heat-tolerant and drought-resistant varieties V6 and V7 were only suitable for very small-scale areas (Figure 11a,c). However, the V6 and V2 varieties were unsuitable for the province in the RCP4.5 and RCP8.5 scenarios, respectively, for 2021–2050.

For 2051–2080, the overall spatial patterns were similar to those for 2021–2050, except for the more dominant representation of heat-tolerant and heat-tolerant and drought-resistant varieties in the RCP4.5 scenario compared with the RCP8.5 scenario (Figure 11b,d). The heat-tolerant variety V2 and the two heat-tolerant and drought-resistant varieties V6 and V7 were unsuitable for the province in the RCP4.5 scenario (Figure 11b). In contrast, in the RCP8.5 scenario, all nine proposed varieties were considered for planting in the province. However, some of the varieties, such as the current variety V1, the heat-tolerant variety V2, the drought-resistant varieties V4 and V5, and the heat-tolerant and drought-resistant varieties V6 and V7, were only suitable for very small-scale areas (Figure 11d). Generally, the heat-tolerant or heat-tolerant and drought-resistant varieties are expected to mitigate

the influences of climate change on winter wheat production in most parts of Jiangsu, unlike the current variety.

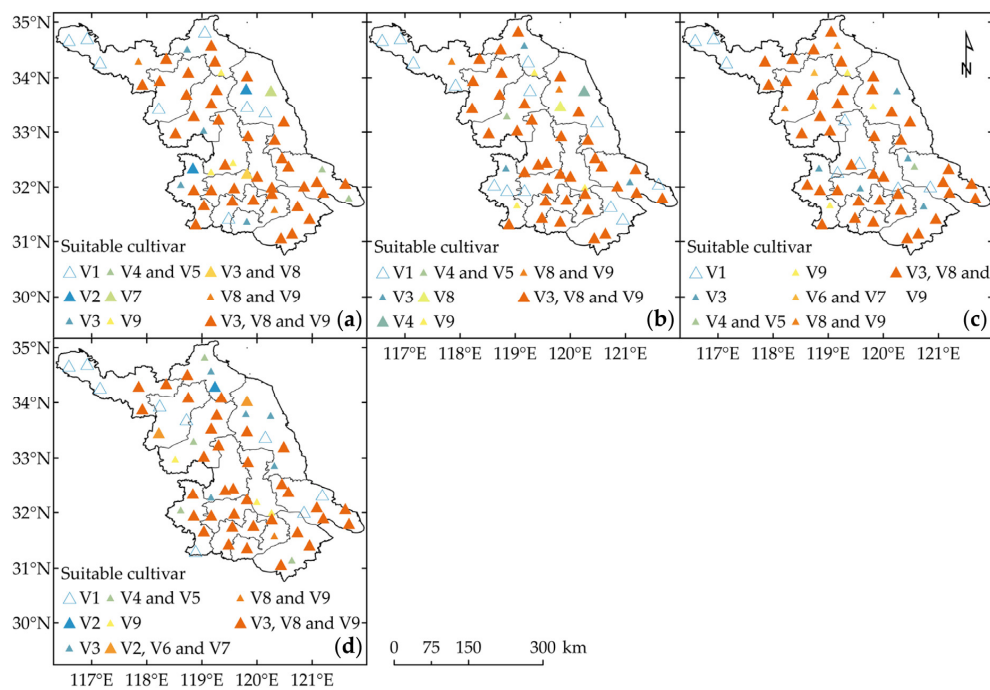


Figure 11. Distributions of cultivar suitability for stable yields: (a) RCP4.5 for 2021–2050; (b) RCP4.5 for 2051–2080; (c) RCP8.5 for 2021–2050; and (d) RCP8.5 for 2051–2080.

After identifying the most suitable cultivars, yield increases were projected in most of the sub-regions, especially in HA, NT, TZ and YC (Figure 12). However, in some sub-regions, such as XZ and NJ, changing the cultivars did not facilitate an obvious yield increase. Similar projections were also obtained in YZ for 2021–2050 in the RCP8.5 scenario (Figure 12c) and in SZ during 2051–2080 in the RCP4.5 scenario (Figure 12b). Although the yield gains projected from the application of the most suitable cultivar were smaller than the yield gains projected from adjusting the sowing dates, it would be appropriate to consider changes in winter wheat variety.

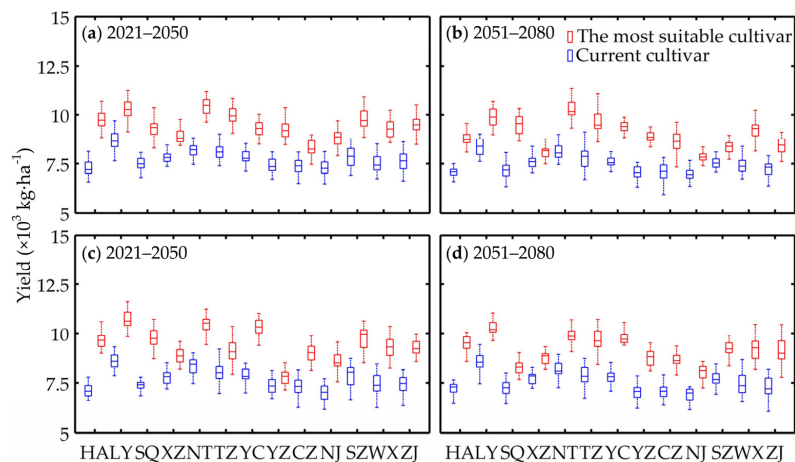


Figure 12. Distribution of the average projected yields after using the identified suitable cultivars in 13 sub-regions in the (a,b) RCP4.5 and (c,d) RCP8.5 scenario. Boxes and whiskers represent the inter-quartile range (between the 25th and 75th percentiles) and maximum and minimum values, and the central mark represents the median.

4. Discussion

This study presents a method for projecting the responses of winter wheat production to chosen adaptation options in Jiangsu, which is a major province in China that is currently experiencing a conflict between economic development and agricultural sustainability. A shorter growing season and more unstable water use efficiency and yields of winter wheat were projected under future climate conditions assuming that the farmers would continue to use the historical cropping patterns.

The temperature increases that will occur with future climate change were projected to result in shorter phenophases. This finding is consistent with the response of winter wheat growth that was projected by Song *et al.* [42]. A suitable GS is required for high production; otherwise, an overly short growing season will cause yield reductions. The WUE was projected to increase slightly, mainly because the relative change of evapotranspiration was much lower than that of the projected yield. This result is similar to the findings of Cuculeanu [11] and Mo *et al.* [43]. However, the WUE was projected to have an unstable tendency with a pronounced negative effect. If only the increases in average yield are considered, the winter wheat production in Jiangsu would benefit from future climates with higher temperatures and radiation levels. However, when the relative change in CV is considered, the yields in many parts of northwestern Jiangsu are projected to become much more unstable in future climate scenarios. Moreover, the CV values that were obtained in this study (approximately 9.9%) were lower than the mean CV value (13.7%) of winter wheat that was calculated in the North China Plain [43]. Thus, our results suggest stable conditions for winter wheat production in Jiangsu. The changes in the winter wheat yields that were simulated during the baseline period are largely consistent with the results of Song *et al.* [5]; however, our study yielded more detailed information because of the abundance of high-resolution data. These data increase our understanding of future trends. This study also presented a paradox; namely, large increases in winter wheat yield in northeastern Jiangsu were simulated in the RCP4.5 and RCP8.5 scenarios, while the winter wheat production in this sub-region was projected to become much more unstable. Considerable attention should be given to this paradox regarding high and stable production in future climate scenarios.

Thus, for policymakers and farmers, rigorous local assessments of adaptation options are required to ensure stable yields. Several studies have recommended using later sowing dates or introducing resistant varieties for winter wheat production in warming climates [11,44,45]. However, these generalized adaptation options are not practical across the entire study region.

Large yield gains characterized by high yields with small CVs for winter wheat were projected from earlier sowing. These gains are consistent with those of previous studies (e.g., [46]); however, in our study, the associated CV index was also introduced as the main criterion of Conditions (a)–(c) as outlined in Section 2.3.2. The results of the sensitivity analysis to different sowing dates yielded a suitable range of sowing dates for each station. The inferior limit was established based on the yield (high) and CV (minimum). The suitable range indicates that planting should be delayed in some parts of northern Jiangsu (e.g., Shuyang and Jianhu) and advanced in some areas of southern Jiangsu (e.g., Wuxi). Sowing dates that are too early for winter wheat production could result in a large number of tillering branches becoming jointed before winter and could lead to potential freezing damage. However, sowing dates that are too late might result in a small number of tillering branches, which would reduce yields. Southworth *et al.* [47] suggested that adaptations in management strategies should be considered when changing sowing dates.

In addition, yield gains were projected from heat-tolerant or heat-tolerant and drought-resistant varieties; thus, the results from the sensitivity analysis of using different cultivars in this study suggest that new wheat cultivars should be introduced, which corresponds with previous conclusions [39]. The heat-tolerant and heat-tolerant and drought-resistant varieties would be suitable in central and southern Jiangsu, and the current cultivar would be more suitable in some areas of the northwestern regions. These results are consistent with the simulated warmer temperatures and lower precipitation in future scenarios. Heat stress can threaten winter wheat at any growth stage [48], and water stress can affect the tillering, booting, and grain-forming stages [49]. Heat-tolerant and drought-resistant varieties

should be the preferred choice in Jiangsu under future climate conditions. This recommendation is consistent with the adaptations that have been proposed for changing maize cultivars in northeastern China [50].

Nevertheless, uncertainties in our assessment are unavoidable, and further assessment of these uncertainties is difficult. The outputs of the climate model contribute to these uncertainties. Most of the climate scenarios were constructed using GCMs, and some of the scenarios are the outputs from mesoscale models that are driven by GCMs [29,51]. Generally, these constructions are validated by comparing the simulated climate elements and observations of the present climate at the annual scale [29]. However, problems occur because crop production, including winter wheat production, is sensitive to seasonal climate changes and because the bias from real climates at monthly scales results in changes in crop development. Even if climate scenarios from multi-models are applied to conduct ensemble assessments, this problem is unavoidable in the absence of bias corrections according to the observations. Thus, as was suggested by Bakker *et al.* [20], it is necessary to correct the shift and variability of the climate scenario before performing the crop simulations. The bias correction method that is proposed in this study mainly consists of a nonlinear transfer function and parameters for variation correction. The corrected daily mean temperature, maximum temperature and minimum temperature were superior to the outputs of RegCM4.0. Biases in precipitation, radiation and evapotranspiration were difficult to correct but were reduced somewhat by using our bias correction method. This method can accommodate the mean and variation shifts, as do other well-documented methods [23,41,52]. However, the assumption that the variation parameters are time-invariant and the relationships between the mean values of observations and historical simulations limit the correction validations. We speculated that a transfer function constructed using mean values at monthly scales might be more effective.

Moreover, the emissions scenarios, local climate and soil conditions explain the uncertainties [53]. In addition, field management, fertilizer and possible damage due to meteorological events, disease, or insect pests, were not considered or determined with ideal values, which also contributed to the uncertainties in our simulations. The results of a recent study [54] that investigated the relative contributions of climate change and technological advances on crop yield are promising for the further study of uncertainties. The main limitation of the present study is the use of a single climate and crop model. However, this negative effect might be reduced for the sensitivity analysis. In addition, our bias correction method was effective for the simulated climate scenarios, reduced the uncertainties that arise from the single climate model and enhanced the credibility of the projections of winter wheat production. Moreover, the application of abundant high-resolution data, including meteorological, crop and soil data, and further calibration of the WOFOST model reduced the uncertainties in the single crop model. The construction of ensemble assessments could be useful. However, as was mentioned above, the quality of each ensemble member would continue to affect the assessment results if a prior bias correction is not carried out, especially when the dispersion between the members is large.

5. Conclusions

The future climate conditions in Jiangsu were projected to affect the winter wheat growing season, water use efficiency and yield in the RCP4.5 and RCP8.5 scenarios. In particular, yield decreases were projected for 2021–2050 and 2051–2080. Adjusting the sowing dates and cultivars was expected to mitigate the influences of climate change on winter wheat production because yield gains were projected from the chosen sowing date and cultivar. However, these two types of adaptation options may not be practical for all sub-regions under the changing climate. Thus, the suitable range of sowing dates and the most suitable variety were identified for each station to obtain high and stable yields. The identified suitable ranges involved earlier sowing dates for the Jianghuai and Huaibei regions than for the regions in southern Jiangsu. In addition, the latest sowing dates should be advanced in some areas of northern Jiangsu and could be delayed in southern Jiangsu. The sensitivity analysis also

suggested that heat-tolerant or heat-tolerant and drought-resistant varieties will be more suitable than the current variety under future climate conditions in this province.

The potential impacts of our study include the application of our regional climate change projections to crop-production planning using coupled agrometeorological and regional climate models as well as higher-level impacts, such as influencing the state's climate-change policies. Further studies should include multiple scenarios and simulations, more extensive model parameterization, and other possible adaptation options.

Acknowledgments: We thank three anonymous reviewers for their expert comments and suggestions, which have improved our manuscript. We also acknowledge the contributions of Wei Xiao from the Yale-NUIST Centre on Atmospheric Environment, Nanjing University of Information Science & Technology. This work was supported by the Climate Change Specific Foundation of China Meteorological Administration (CCSF201318), the Funding of Jiangsu Innovation Program for Graduate Education (CXZZ12_0503), the Research Fund for the Public Sector of China (GYHY201506018 and GYHY201306046), the Open Foundation of the Jiangsu Key Laboratory of Agricultural Meteorology (JKLAM201202) and the Project funded by Norway for Improving Weather Information Management in East Africa for effective service provision through the application of suitable ICTs (UGA-13/0018).

Author Contributions: This work was completed as a collaboration among all of the authors. Sulin Tao conducted the main part of the study under the guidance of Shuanghe Shen. Numerical experiments were designed by Sulin Tao and Yuhong Li and performed with the help of Qi Wang. Ping Gao provided the experimental data and revised the manuscript with the help of Isaac Mugume.

Conflicts of Interest: The authors declare no conflict of interests regarding the publication of this paper.

Appendix

A Bias Correction (BC) Method for Model-Simulated Climate Data

The main steps of our bias correction method are detailed below.

- (i) First, a nonlinear transfer function between the mean values of historical simulations and observations was determined for each ten-day period of the year. This function was constructed using a quadratic regression equation as follows:

$$F(X) = c_1 X^2 + c_2 X + c_3, \quad (\text{A1})$$

where X and F are the predictor and predictand, respectively. Our experiments suggested this quadratic form of transfer function because linear functions explained only a small fraction of the observed climate variability and cubic or higher order transfer functions provided poor approximations (e.g., extremely large values) for the highly oscillatory feature.

The coefficients c_1 , c_2 and c_3 were determined using historical simulations and observations using the least squares method. For this purpose, the mean values of the simulated data during every ten-day period of the year, $k^{-1} \sum_{i=1}^k x_i^s$, were defined as the predictor, and the mean values of observed data, $k^{-1} \sum_{i=1}^k x_i^o$, were specified for the value of F . Here, x_i^s and x_i^o are the simulation and observation sequences, respectively; k indicates the number of days during a ten-day period and is 8, 9, 10 or 11 according to the different months of different years; and i is the ordinal day.

The historical simulations in this study were generated from RegCM4.0 coupled with BCC_CSM1.1 during the baseline period of 1961–1990. Next, these data were interpolated to the locations of the meteorological sites by using bilinear interpolation to prepare parallel data sequences. One-to-one mapping between historical simulations and climatic observations does not exist because no dependent variable for observed radiation has been reported. Extra simulations were performed to prepare daily global radiation by using an Angström-like model.

- (ii) Second, the mean correction was applied to the uncorrected daily value x_i as follows:

$$\begin{aligned}\dot{x}_i &= F \left(k^{-1} \sum_{i=1}^k x_i \right) + \left(x_i - k^{-1} \sum_{i=1}^k x_i \right) \\ &= \left[c_1 \left(k^{-1} \sum_{i=1}^k x_i \right)^2 + c_2 \left(k^{-1} \sum_{i=1}^k x_i \right) + c_3 \right] + \left(x_i - k^{-1} \sum_{i=1}^k x_i \right) \\ &= x_i + c_1 \left(k^{-1} \sum_{i=1}^k x_i \right)^2 + (c_2 - 1) \left(k^{-1} \sum_{i=1}^k x_i \right) + c_3,\end{aligned}\quad (\text{A2})$$

where \dot{x}_i is an intermediate variable after mean correction.

- (iii) Third, the parameter λ was used for variation correction and was determined for each ten-day period of the year because the direct application of quadratic regression models would reduce the variability between the variable \dot{x}_i and the original predictor x_i . This parameter was determined by the intermediate variable \dot{x}_i and the mean value of the variance of the observation x_i^o during the baseline conditions as follows:

$$\lambda = \left\{ \left[M^{-1} \sum_{m=1}^M \text{var} (x_i^o)_m \right] / \text{var} (\dot{x}_i) \right\}^{1/2}. \quad (\text{A3})$$

The symbol $\text{var}(\cdot)$ represents the calculated variance and M is the total number of years during the baseline period, which was 30 in this study.

- (iv) Finally, the variation correction was applied as follows:

$$\ddot{x}_i = \lambda \dot{x}_i + (1 - \lambda) \left(k^{-1} \sum_{i=1}^k \dot{x}_i \right), \quad (\text{A4})$$

where \ddot{x}_i is the variable after variation correction and is the final corrected value.

Thus, our bias correction method consisted of corrections for the mean and variation. For example, here we consider the bias correction for daily mean temperature in Nanjing. The bias correction model for the daily mean temperature in the first ten-day period of January was constructed as follows:

$$\ddot{T}_i = \lambda \dot{T}_i + (1 - \lambda) \left(k^{-1} \sum_{i=1}^k \dot{T}_i \right), \quad (\text{A5})$$

with

$$\dot{T}_i = T_i + c_1 \left(k^{-1} \sum_{i=1}^k T_i \right)^2 + (c_2 - 1) \left(k^{-1} \sum_{i=1}^k T_i \right) + c_3, \quad (\text{A6})$$

$$\lambda = \left\{ \left[M^{-1} \sum_{m=1}^M \text{var} (T_i^o)_m \right] / \text{var} (\dot{T}_i) \right\}^{1/2}, \quad (\text{A7})$$

$$c_1 = -1.41 \times 10^{-2}, c_2 = 0, c_3 = 2.32, k = 10, \text{ and } M = 30, \quad (\text{A8})$$

where \ddot{T}_i and T_i are the corrected and uncorrected temperatures on the i th day, respectively. \dot{T}_i is the intermediate variable, and T_i^o is the observed baseline temperature. The c_1 , c_2 and c_3 coefficients were estimated using the least squares method with historical simulations and the corresponding

observations from 1961 to 1990. Bias Correction Models (2–4) were constructed for the other climate elements and other sites using the same method.

References

- Rosenzweig, C.; Iglesias, A.; Yang, X.B.; Epstein, P.R.; Chivian, E. Climate change and extreme weather events; implications for food production, plant diseases, and pests. *Glob. Chang. Hum. Health* **2001**, *2*, 90–104. [[CrossRef](#)]
- Tao, F.; Yokozawa, M.; Xu, Y.; Hayashi, Y.; Zhang, Z. Climate changes and trends in phenology and yields of field crops in China, 1981–2000. *Agric. For. Meteorol.* **2006**, *138*, 82–92. [[CrossRef](#)]
- Nicholls, N. Increased Australian wheat yield due to recent climate trends. *Nature* **1997**, *387*, 484–485. [[CrossRef](#)]
- Semenov, M.A.; Porter, J.R. Climatic variability and the modelling of crop yields. *Agric. For. Meteorol.* **1995**, *73*, 265–283. [[CrossRef](#)]
- Song, Y.; Chen, D.; Dong, W. Influence of climate on winter wheat productivity in different climate regions of China, 1961–2000. *Clim. Res.* **2006**, *32*, 219–227. [[CrossRef](#)]
- Vashisht, B.B.; Mulla, D.J.; Jalota, S.K.; Kaur, S.; Kaur, H.; Singh, S. Productivity of rainfed wheat as affected by climate change scenario in northeastern Punjab, India. *Reg. Environ. Chang.* **2013**, *13*, 989–998. [[CrossRef](#)]
- De Wit, A.; Duveiller, G.; Defourny, P. Estimating regional winter wheat yield with WOFOST through the assimilation of green area index retrieved from MODIS observations. *Agric. For. Meteorol.* **2012**, *164*, 39–52. [[CrossRef](#)]
- Riha, S.J.; Wilks, D.S.; Simoens, P. Impact of temperature and precipitation variability on crop model predictions. *Clim. Chang.* **1996**, *32*, 293–311. [[CrossRef](#)]
- Hulme, M.; Barrow, E.M.; Arnell, N.W.; Harrison, P.A.; Johns, T.C.; Downing, T.E. Relative impacts of human-induced climate change and natural climate variability. *Nature* **1999**, *397*, 688–691. [[CrossRef](#)]
- Semenov, M.A. Impacts of climate change on wheat in England and Wales. *J. R. Soc. Interface* **2009**, *6*, 343–350. [[CrossRef](#)] [[PubMed](#)]
- Cuculeanu, V.; Marica, A.; Simota, C. Climate change impact on agricultural crops and adaptation options in Romania. *Clim. Res.* **1999**, *12*, 153–160. [[CrossRef](#)]
- Torriani, D.; Calanca, P.L.; Schmid, S.; Beniston, M.; Fuhrer, J. Potential effects of changes in mean climate and climate variability on the yield of winter and spring crops in Switzerland. *Clim. Res.* **2007**, *34*, 59–69. [[CrossRef](#)]
- Alexandrov, V.A.; Hoogenboom, G. The impact of climate variability and change on crop yield in Bulgaria. *Agric. For. Meteorol.* **2000**, *104*, 315–327. [[CrossRef](#)]
- Luo, Q.; Bellotti, W.; Williams, M.; Wang, E. Adaptation to climate change of wheat growing in south Australia: Analysis of management and breeding strategies. *Agric. Ecosyst. Environ.* **2009**, *129*, 261–267. [[CrossRef](#)]
- Olesen, J.E.; Trnka, M.; Kersebaum, K.C.; Skjelvåg, A.O.; Seguin, B.; Peltonen-Sainio, P.; Rossi, F.; Kozyra, J.; Micale, F. Impacts and adaptation of European crop production systems to climate change. *Eur. J. Agron.* **2011**, *34*, 96–112. [[CrossRef](#)]
- Bradshaw, B.; Dolan, H.; Smit, B. Farm-level adaptation to climatic variability and change: Crop diversification in the Canadian prairies. *Clim. Chang.* **2004**, *67*, 119–141. [[CrossRef](#)]
- Xu, Z.; Yang, Z.-L. An improved dynamical downscaling method with GCM bias corrections and its validation with 30 years of climate simulations. *J. Clim.* **2012**, *25*, 6271–6286. [[CrossRef](#)]
- Xu, Z.; Yang, Z.-L. A new dynamical downscaling approach with GCM bias corrections and spectral nudging. *J. Geophys. Res.* **2015**, *120*, 3063–3084. [[CrossRef](#)]
- Huth, R. Statistical downscaling in central Europe: Evaluation of methods and potential predictors. *Clim. Res.* **1999**, *13*, 91–101. [[CrossRef](#)]
- Bakker, A.M.R.; Bessembinder, J.J.E.; de Wit, A.J.W.; van den Hurk, B.J.J.M.; Hoek, S.B. Exploring the efficiency of bias corrections of regional climate model output for the assessment of future crop yields in Europe. *Reg. Environ. Chang.* **2014**, *14*, 865–877. [[CrossRef](#)]

21. Sun, W.; Huang, Y. Global warming over the period 1961–2008 did not increase high-temperature stress but did reduce low-temperature stress in irrigated rice across China. *Agric. For. Meteorol.* **2011**, *151*, 1193–1201. [[CrossRef](#)]
22. Mai, M.; Zha, S.-P.; Zhu, B.; Xu, L. Agro-climatic resource zoning in Jiangsu province. *Meteorol. Environ. Res.* **2010**, *1*, 59–63.
23. Ajaaj, A.A.; Mishra, A.K.; Khan, A.A. Comparison of bias correction techniques for GPCC rainfall data in semi-arid climate. *Stoch. Environ. Res. Risk Assess.* **2015**. [[CrossRef](#)]
24. Zhang, H.-F.; Zhou, S.-L.; Wu, S.-H.; Zheng, G.-H.; Hua, S.; Li, L. Temporal and spatial variation of grain production in Jiangsu province and its influencing factors. *J. Nat. Resour.* **2011**, *26*, 319–327. (In Chinese)
25. Li, S.; Wheeler, T.; Challinor, A.; Lin, E.; Ju, H.; Xu, Y. The observed relationships between wheat and climate in China. *Agric. For. Meteorol.* **2010**, *150*, 1412–1419. [[CrossRef](#)]
26. Van Vuuren, D.P.; Edmonds, J.; Kainuma, M.; Riahi, K.; Thomson, A.; Hibbard, K.; Hurtt, G.C.; Kram, T.; Krey, V.; Lamarque, J.-F.; *et al.* The representative concentration pathways: An overview. *Clim. Chang.* **2011**. [[CrossRef](#)]
27. Riahi, K.; Rao, S.; Krey, V.; Cho, C.; Chirkov, V.; Fischer, G.; Kindermann, G.; Nakicenovic, N.; Rafaj, P. RCP8.5—A scenario of comparatively high greenhouse gas emissions. *Clim. Chang.* **2011**, *109*, 33–57. [[CrossRef](#)]
28. Thomson, A.M.; Calvin, K.V.; Smith, S.J.; Kyle, G.P.; Volke, A.; Patel, P.; Delgado-Arias, S.; Bond-Lamberty, B.; Wise, M.A.; Clarke, L.E.; *et al.* RCP4.5: A pathway for stabilization of radiative forcing by 2100. *Clim. Chang.* **2011**, *109*, 77–94. [[CrossRef](#)]
29. Gao, X.J.; Wang, M.-L.; Giorgi, F. Climate change over China in the 21st century as simulated by BCC_CSM1.1-RegCM4.0. *Atmos. Ocean. Sci. Lett.* **2013**, *6*, 381–386.
30. Food and Agriculture Organization of the United Nations; International Institute for Applied Systems Analysis; World Soil Information; Institute of Soil Science—Chinese Academy of Sciences; Joint Research Centre of the European Commission. *Harmonized World Soil Database*; version 1.0; FAO: Rome, Italy; IIASA: Laxenburg, Austria, 2008.
31. Diepen, C.V.; Wolf, J.; Keulen, H.V.; Rappoldt, C. WOFOST: A simulation model of crop production. *Soil Use Manag.* **1989**, *5*, 16–24. [[CrossRef](#)]
32. Boogaard, H.L.; van Diepen, C.A.; Rötter, R.P.; Cabrera, J.M.C.A.; van Laar, H.H. *WOFOST 7.1: User's Guide for the WOFOST 7.1 Crop Growth Simulation Model and WOFOST Control Center 1.5*; DLO Winand Staring Centre: Wageningen, The Netherlands, 1998.
33. Palosuo, T.; Kersebaum, K.C.; Angulo, C.; Hlavinka, P.; Moriondo, M.; Olesen, J.E.; Patil, R.H.; Ruget, F.; Rumbaur, C.; Takáč, J.; *et al.* Simulation of winter wheat yield and its variability in different climates of Europe: A comparison of eight crop growth models. *Eur. J. Agron.* **2011**, *35*, 103–114. [[CrossRef](#)]
34. Huang, J.; Tian, L.; Liang, S.; Ma, H.; Becker-Reshef, I.; Huang, Y.; Su, W.; Zhang, X.; Zhu, D.; Wu, W. Improving winter wheat yield estimation by assimilation of the leaf area index from Landsat TM and MODIS data into the WOFOST model. *Agric. For. Meteorol.* **2015**, *204*, 106–121. [[CrossRef](#)]
35. Li, Y.; Kinzelbach, W.; Zhou, J.; Cheng, G.D.; Li, X. Modelling irrigated maize with a combination of coupled-model simulation and uncertainty analysis, in the northwest of China. *Hydrol. Earth Syst. Sci.* **2012**, *16*, 1465–1480. [[CrossRef](#)]
36. Ma, H.; Huang, J.; Zhu, D.; Liu, J.; Su, W.; Zhang, C.; Fan, J. Estimating regional winter wheat yield by assimilation of time series of HJ-1 CCD NDVI into WOFOST-ACRM model with ensemble Kalman filter. *Math. Comput. Model.* **2013**, *58*, 759–770. [[CrossRef](#)]
37. Diepen, C.V.; Rappoldt, C.; Wolf, J.; Keulen, H.V. *Crop Growth Simulation Model WOFOST*; version 4.1; Centre for World Food Studies: Wageningen, The Netherlands, 1988.
38. Saxton, K.E.; Willey, P.H. The SPAW model for agricultural field and pond hydrologic simulation. In *Watershed Models*; Singh, V.P., Frevert, D.K., Eds.; CRC Press: Boca Raton, FL, USA, 2006; pp. 401–435.
39. Ortiz, R.; Sayre, K.D.; Govaerts, B.; Gupta, R.; Subbarao, G.V.; Ban, T.; Hodson, D.; Dixon, J.M.; Ortiz-Monasterio, J.I.; Reynolds, M. Climate change: Can wheat beat the heat? *Agric. Ecosyst. Environ.* **2008**, *126*, 46–58. [[CrossRef](#)]
40. Schonfeld, M.A.; Johnson, R.C.; Carver, B.F.; Mornhinweg, D.W. Water relations in winter wheat as drought resistance indicators. *Crop Sci.* **1988**, *28*, 526–531. [[CrossRef](#)]

41. Piani, C.; Haerter, J.O.; Coppola, E. Statistical bias correction for daily precipitation in regional climate models over Europe. *Theor. Appl. Climatol.* **2010**, *99*, 187–192. [[CrossRef](#)]
42. Song, Y.-L.; Chen, D.-L.; Liu, Y.-J.; Xu, Y. The influence of climate change on winter wheat during 2012–2100 under A2 and A1B scenarios in China. *Adv. Clim. Chang. Res.* **2012**, *3*, 138–146.
43. Mo, X.; Liu, S.; Lin, Z.; Guo, R. Regional crop yield, water consumption and water use efficiency and their responses to climate change in the North China Plain. *Agric. Ecosyst. Environ.* **2009**, *134*, 67–78. [[CrossRef](#)]
44. Xiao, D.; Tao, F.; Liu, Y.; Shi, W.; Wang, M.; Liu, F.; Zhang, S.; Zhu, Z. Observed changes in winter wheat phenology in the North China Plain for 1981–2009. *Int. J. Biometeorol.* **2013**, *57*, 275–285. [[CrossRef](#)] [[PubMed](#)]
45. He, L.; Asseng, S.; Zhao, G.; Wu, D.; Yang, X.; Zhuang, W.; Ning, J.; Yu, Q. Impacts of recent climate warming, cultivar changes, and crop management on winter wheat phenology across the Loess Plateau of China. *Agric. For. Meteorol.* **2015**, *200*, 135–143. [[CrossRef](#)]
46. Van Oort, P.A.J.; Timmermans, B.G.H.; van Swaaij, A.C.P.M. Why farmers' sowing dates hardly change when temperature rises. *Eur. J. Agron.* **2012**, *40*, 102–111. [[CrossRef](#)]
47. Southworth, J.; Pfeifer, R.A.; Habeck, M.; Randolph, J.C.; Doering, O.C.; Rao, D.G. Sensitivity of winter wheat yields in the midwestern United States to future changes in climate, climate variability, and CO₂ fertilization. *Clim. Res.* **2002**, *22*, 73–86. [[CrossRef](#)]
48. Cossani, C.M.; Reynolds, M.P. Physiological traits for improving heat tolerance in wheat. *Plant Physiol.* **2012**, *160*, 1710–1718. [[CrossRef](#)] [[PubMed](#)]
49. Mogensen, V.O.; Jensen, H.E.; Rab, M.A. Grain yield, yield components, drought sensitivity and water use efficiency of spring wheat subjected to water stress at various growth stages. *Irrig. Sci.* **1985**, *6*, 131–140. [[CrossRef](#)]
50. Xu, Y.; Guo, J.; Zhao, J.; Mu, J. Scenario analysis on the adaptation of different maize varieties to future climate change in northeast China. *J. Meteorol. Res.* **2014**, *28*, 469–480. [[CrossRef](#)]
51. Semenov, M.A.; Wolf, J.; Evans, L.G.; Eckersten, H.; Iglesias, A. Comparison of wheat simulation models under climate change. II: Application of climate change scenarios. *Clim. Res.* **1996**, *7*, 271–281. [[CrossRef](#)]
52. Piani, C.; Weedon, G.P.; Best, M.; Gomes, S.M.; Viterbo, P.; Hagemann, S.; Haerter, J.O. Statistical bias correction of global simulated daily precipitation and temperature for the application of hydrological models. *J. Hydrol.* **2010**, *395*, 199–215. [[CrossRef](#)]
53. Olesen, J.E.; Carter, T.R.; Díaz-Ambrona, C.H.; Fronzek, S.; Heidmann, T.; Hickler, T.; Holt, T.; Minguéz, M.I.; Morales, P.; Palutikof, J.P.; *et al.* Uncertainties in projected impacts of climate change on European agriculture and terrestrial ecosystems based on scenarios from regional climate models. *Clim. Chang.* **2007**, *81*, 123–143. [[CrossRef](#)]
54. Guo, J.; Zhao, J.; Wu, D.; Mu, J.; Xu, Y. Attribution of maize yield increase in China to climate change and technological advancement between 1980 and 2010. *J. Meteorol. Res.* **2014**, *28*, 1168–1181. [[CrossRef](#)]
55. Chen, R.; Ersi, K.; Yang, J.; Lu, S.; Zhao, W. Validation of five global radiation models with measured daily data in China. *Energ. Convers. Manag.* **2004**, *45*, 1759–1769. [[CrossRef](#)]

